Emergent QED$_3$ from half-filled flat Chern bands

Xue-Yang Song [⬡],[*] Hart Goldman [⬡],[*] and Liang Fu

Department of Physics, Massachusetts Institute of Technology, Cambridge, Massachusetts 02139, USA

Recently, two-dimensional Dirac materials patterned with a superlattice structure have emerged as a rich platform for exploring correlated and topological quantum matter. In this paper, we propose that by subjecting Dirac electrons on a particle-hole symmetric topological insulator (TI) surface to a periodic magnetic field with triangular lattice symmetry, it is possible to realize a *quantum critical phase* of $N_f = 3$ Dirac fermion species strongly coupled to an emergent gauge field, or 2+1-D quantum electrodynamics (QED$_3$). We demonstrate explicitly that the QED$_3$ phase naturally arises from a Dirac composite fermion (CF) picture, where the periodic magnetic field manifests as a periodic CF potential and transforms the CF Fermi surface into gapless Fermi points. We further show that by breaking the particle-hole symmetry of the TI surface—either by doping or by introducing a periodic electrostatic potential with zero mean—our quantum critical phase gives way to a sequence of fractional Chern insulator phases. Our theory illustrates the rich menagerie of quantum phases possible around half filling of a flat Chern band.

I. INTRODUCTION

The unprecedented tunability of two-dimensional (2D) van der Waals materials has led to opportunities to explore unique quantum phases of matter. In particular, a plethora of correlated and topological electron states have been found by engineering 2D systems with a superlattice structure. Major examples include moiré potentials established by stacking 2D materials with a twist angle between layers or a lattice mismatch [1–6], spatially varying strains [7,8], and buckling in graphene sheets [9]. The superlattice patterning of these materials commonly provides a spatial modulation at the length scale of 10 nm, which can give rise to flat bands hosting strong interaction effects.

In the presence of Coulomb interactions, partially filled flat Chern bands at odd-denominator filling fractions can support fractional Chern insulators (FCIs) [10–16]. Like ordinary fractional quantum Hall (FQH) phases, FCIs exhibit a fractionally quantized Hall conductivity, topological order, and fractional excitations, but enriched with the symmetry of the periodic lattice. The search for FCIs in 2D materials has garnered much recent experimental attention [17,18].

Less explored is the case of flat Chern bands at half filling. Ordinary Landau levels (LLs) in a uniform magnetic field are experimentally observed to host a range of correlated phases at half filling, depending on the LL index, n. These include the composite Fermi liquid (CFL) ($n = 0$) [19,20], a non-Abelian FQH state ($n = 1$) [21–24], and charge ordered states (higher n) [25–30]. We are therefore driven to ask: Can topological flat bands beyond LLs support additional types of quantum phases at half filling? If so, in what material platforms can they be found?

In this paper, we demonstrate the emergence of an exotic *quantum critical phase* in half-filled flat Chern bands, and we propose a realistic material platform for its physical realization. This phase can be described in terms of $N_f = 3$ species of emergent Dirac fermions strongly interacting through a dynamical U(1) gauge field or $2 + 1$-D quantum electrodynamics (QED$_3$). As a strongly interacting conformal field theory, many of the universal properties of QED$_3$ are unknown outside of large-N_f limits, and numerical methods [31–38] have thus far made limited progress, making the possibility of its physical realization all the more tantalizing.

We show that the quantum critical QED$_3$ state can be realized from a system of 2D Dirac electrons subject to a periodic magnetic field with triangular lattice symmetry and two flux quanta per unit cell. In the limit of a uniform magnetic field and at charge neutrality, the $n = 0$ LL is half filled, and, in the presence of Coulomb interactions, the ground state is a CFL. When a periodic modulation in the magnetic field is introduced, the composite fermions (CFs) experience a periodic electric potential, leading to the formation of CF bands. By solving the CF band structure at mean-field level, we find that massless Dirac cones appear at three M points of the Brillouin zone (BZ). For the case of two flux quanta per unit cell, these emergent Dirac cones cross the Fermi level, i.e., the CF Fermi surface is transformed into three CF Fermi points by periodic field modulation. The low-energy physics of the resulting quantum critical state is thus governed by $N_f = 3$ QED$_3$ (see Fig. 1).

Crucial to our construction is the particle-hole symmetry of the physical electrons at half filling of the Chern band, which protects the emergent Dirac fermions of our QED$_3$ phase from becoming gapped. We also require the electronic Chern band to be sufficiently flat: A large enough bandwidth will instead
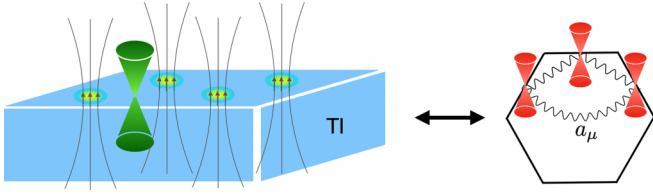
FIG. 1. The schematic setup: Topological insulator surface under a periodic magnetic field, forming a triangular vortex lattice in our case, which could arise from proximity to type-II superconductors. The low-energy theory consists of three Dirac fermions interacting with photons (QED$_3$).

favor an ordinary Fermi liquid state at half filling. These two conditions are simultaneously satisfied in 2D Dirac electron systems at charge neutrality, such as topological insulator (TI) surface states, subject to a periodic magnetic field.

We further show that when the electronic particle-hole symmetry is broken with a periodic electrostatic potential, the QED$_3$ quantum critical phase gives way to FCI phases with topological orders of $\nu = \pm 1/3$ Laughlin states, consistent with earlier studies on FCI phase transitions [39]. We also find by doping away from half filling a Jain sequence of further FCI phases. Dirac materials in a periodic magnetic field are thus a simple and robust setup realizing both QED$_3$ and FCI phases from a half-filled flat Chern band.

II. SETUP

We begin by considering the TI surface in a uniform magnetic field. The surface of the TI supports a single Dirac electron, Ψ, with action

$$S_\Psi = \int_{t,\boldsymbol{x}} i\bar{\Psi}(\partial_\mu - iA_\mu)\gamma^\mu\Psi, \qquad (1)$$

where A_μ is the background electromagnetic (EM) field, $\gamma^\mu = (\sigma^z, i\sigma^x, i\sigma^y)$ are the Dirac gamma matrices, and we take the Dirac electrons' velocity to be $v = 1$. Throughout the paper, we will use boldface to denote spatial vectors, as well as the notation $\int_{t,\boldsymbol{x}} \equiv \int dt\, d^2\boldsymbol{x}$. We also work in units of $\hbar = c = k_B = 1$ unless otherwise noted. In the presence of a uniform magnetic field, $B_0 = \nabla \times A_{(0)}$, $A_{(0)} = \frac{B_0}{2}(y, -x)$, time-reversal symmetry ($\mathcal{T}$) is broken while particle-hole symmetry ($\mathcal{PH}$) [40] remains intact. Consequently, the Dirac electrons form positive and negative-energy LLs. At charge neutrality, the particle-hole symmetry $\mathcal{PH}$ (which exchanges empty and filled states) guarantees that the $n = 0$ LL at zero energy is exactly at half filling for any B_0. Note that realistic TI materials will break $\mathcal{PH}$ through a Zeeman term, $gB_0\bar{\Psi}\Psi$. For the physics of emergent QED$_3$ to be accessible without fine-tuning, we will require $\mathcal{PH}$ to be exact and thus assume $g = 0$.

It is well-known that in the presence of Coulomb interaction, the half-filled $n = 0$ LL is a strongly correlated metallic phase known as a CFL [19,20,41]. The existence of the CFL can be explained using flux attachment [42–45], in which each electron is transmuted into a CF via adiabatic attachment of two flux quanta. Attaching flux screens the external magnetic field completely, allowing the CFs to form a Fermi surface coupled to a fluctuating U(1) gauge field. Although

the traditional flux attachment procedure breaks $\mathcal{PH}$—one must decide whether to attach flux to electrons or holes—Son proposed a CFL theory [46] where $\mathcal{PH}$ is manifest:

$$S_\psi = \int_{t,\boldsymbol{x}} \left[i\bar{\psi}(\partial_\mu - ia_\mu)\gamma^\mu\psi + \frac{1}{4\pi}Ada \right]. \qquad (2)$$

Here the CFs, ψ, are Dirac fermions coupled to a fluctuating U(1) gauge field, a_μ, and we have defined the emergent magnetic field, $b_* = \nabla \times \boldsymbol{a}$. From the point of view of the Dirac CFL, the physical electrons in the $n = 0$ LL are double vortices of the emergent gauge field [47–54],

$$\rho_e = \Psi^\dagger\Psi \leftrightarrow \frac{1}{4\pi}b_*, \quad J_e^i = \bar{\Psi}\gamma^i\Psi \leftrightarrow \frac{1}{4\pi}\varepsilon^{ij}e_j, \qquad (3)$$

where $e_i = \partial_i a_t - \partial_t a_i$. Similarly, like in the well-known boson-vortex duality [55–57], the Dirac CFs are vortices of the physical magnetic field: a_t acts as a Lagrange multiplier fixing the CF density, $\rho_\psi = \psi^\dagger\psi$,

$$\rho_\psi = \psi^\dagger\psi = -\frac{1}{2}\frac{B}{2\pi}, \qquad (4)$$

meaning that a single CF corresponds to two flux quanta. The CFL thus has a circular Fermi surface fixed by the external magnetic field, with Fermi wave vector, $k_F = \sqrt{|4\pi\,\rho_\psi|} = \sqrt{|B|}$. For a recent review of the physics of the CFL in half-filled LLs and a comparison of the Dirac CFL theory with the nonrelativistic flux attachment approach, see Ref. [41].

Importantly, the microscopic $\mathcal{PH}$ symmetry of the half-filled LL problem appears as a time-reversal symmetry of the Dirac CFs [46], which feel no magnetic field. It acts on the Dirac CF variables as

$$\mathcal{PH} : \psi \to -i\sigma^y\psi, \quad (a_0, a_i) \to (a_0, -a_i). \qquad (5)$$

For clarity below, we will denote this symmetry as $\mathcal{T}_{\mathrm{CF}}$ when discussing its action in the context of the Dirac CF theory.

III. EMERGENT $N_f = 3$ QED$_3$ FROM PERIODIC MAGNETIC FIELD

We proceed to consider the case where the TI surface is subject to a periodic magnetic field. One way such a setup can be established is by placing TI film on top of a type-II superconductor, where an external magnetic field, H, induces an Abrikosov vortex lattice, which in turn periodically modulates the magnetic field, B, felt by the TI. However, in such a setup the flux per unit cell is fixed to the superconducting flux quantum, $h/2e$, rather than the desired case of $2h/e$. Alternatively, a periodic magnetic field can be induced by an array of micromagnets [58,59]. As shown by a recent study [60], in Dirac electron systems under a periodic B field, there remains a perfectly flat Chern band at zero energy, which leads to competing FCI and Wigner crystal states at odd-denominator filling fractions. Our paper studies the case of half filling, which corresponds to charge neutrality. It is important to note that we assume the particle-hole symmetry $\mathcal{PH}$ remains exact even when the magnetic field is nonuniform.
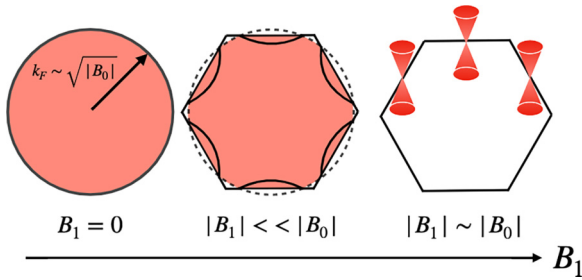
FIG. 2. The evolution of the CF Fermi surface at unit filling of the periodic potential. As the strength of the periodic modulation, $|B_1|$ is increased, the CF bands fold at the Brillouin zone edge, and the original circular Fermi surface is deformed. When $|B_1|/|B_0| \sim O(1)$, three isolated Dirac cones emerge at the Fermi energy.

We now consider a magnetic field with both uniform and spatially oscillating components:

$$B(\boldsymbol{x}) = B_0 + 2B_1 \sum_{n=1}^{6} \cos(\boldsymbol{Q}_n \cdot \boldsymbol{x}). \tag{6}$$

Here the oscillatory component, which is a two-dimensional periodic function, defines a triangular lattice with lattice constant $\mathfrak{a}$. $\boldsymbol{Q}_n = \frac{4\pi}{\sqrt{3}\,\mathfrak{a}}(\sin(\frac{\pi(n-1)}{3}), \cos(\frac{\pi(n-1)}{3}))$, $n = 1, \dots, 6$, are the reciprocal lattice vectors. The CF filling per triangular lattice unit cell is equal to half the number of flux quanta per unit cell, by Eq. (4).

In the Dirac CF variables, a slowly varying magnetic field leads to a slowly varying CF density, $\rho_\psi(\boldsymbol{x}) = -B(\boldsymbol{x})/4\pi$. Rather than implement this identity as a constraint, it is convenient to instead enforce this relation on average by introducing a scalar potential for the CFs of the same symmetry as the magnetic field $B(\boldsymbol{x})$:

$$S_V = -\int_{t,\boldsymbol{x}} V_{\mathrm{CF}}(\boldsymbol{x})\, \psi^\dagger \psi(t, \boldsymbol{x}),$$

$$V_{\mathrm{CF}}(\boldsymbol{x}) = \mu_0 + 2V_1 \sum_{n=1}^{6} \cos(\boldsymbol{Q}_n \cdot \boldsymbol{x}). \tag{7}$$

The coefficient, $V_1 \propto \ell_{B_0} B_1/4\pi$, $\ell_{B_0} = 1/\sqrt{B_0}$, are self-consistently determined by enforcing Eq. (4) for the mean density, $\langle \rho_\psi \rangle$ (see Appendix B).[1] The full action for the CFs we will consider is therefore the sum of Eq. (2) with S_V. Next we derive the low-energy, long-wavelength theory for the CFs.

The presence of the periodic potential $V_{\mathrm{CF}}(\boldsymbol{x})$ leads to band folding. When the periodic potential in Eq. (7) is made sufficiently strong, $B_1/B_0 \sim O(1)$, the mean-field Dirac CF band structure exhibits three Dirac cones connecting the first and second bands at $E > 0$ (see Fig. 2). These Dirac cones are degenerate and located at the M points of the BZ, consistent with the C_6 lattice rotation symmetry and the CF time-reversal symmetry, $\mathcal{T}_{\mathrm{CF}}$. This CF band structure is depicted in the top panel of Fig. 3, which is obtained by solving the mean-field

_____

[1]This procedure is valid by the equivalence of thermodynamic ensembles: We have passed from the canonical to the grand canonical formulation of the CF theory.
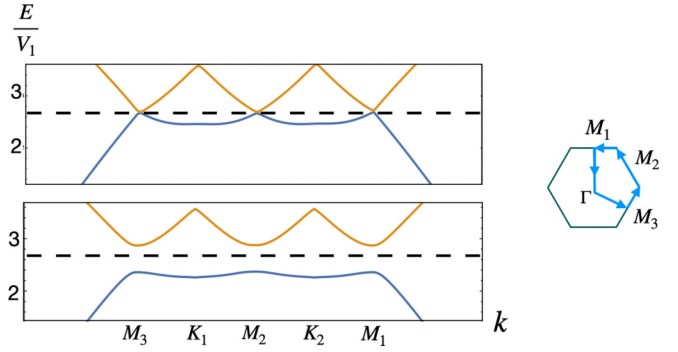
FIG. 3. The dispersion of the CFs under a periodic potential, Eq. (7), with $V_1 = 2/(\sqrt{3}\mathfrak{a})$. Top: When the electronic $\mathcal{PH}$ symmetry is enforced, three Dirac cones appear in the CF spectrum at the M points of the BZ. At filling, $f = 1$, the chemical potential (dashed line) crosses each of the Dirac points. Right: There are three Dirac cones along the plotted trajectory at the Fermi energy. Bottom: Introducing a commensurate, periodic scalar potential for the electrons (magnetic field for the CFs) breaks $\mathcal{PH}$ and causes a gap to open.

CF Hamiltonian numerically (see Appendix A). Of particular interest to us is the case of unit filling of the triangular lattice, which we denote $f = 1$. In this case, there are two flux quanta—hence a single CF—at each triangular lattice unit cell. Consequently, the Fermi level of the CFs is exactly at the Dirac points, i.e., the original CF Fermi surface is transformed into three Fermi points by the periodic modulation of magnetic field. Reintroducing gauge fluctuations, the theory then finds itself in an exotic *quantum critical phase* governed by QED$_3$ with $N_f = 3$ fermion species.

We now explicitly calculate the CF dispersion near the BZ M points to leading order in the periodic potential [61]. Without loss of generality, we focus on the points $\pm \boldsymbol{M}_1 = \pm(0, 2\pi/(\sqrt{3}\mathfrak{a}))$ and consider the mean-field CF Dirac Hamiltonian obtained from the sum of Eqs. (2) and (7), neglecting gauge fluctuations, $\langle a_\mu \rangle = 0$. In the absence of the periodic potential term, the eigenspinors of the CF Dirac Hamiltonian about the M_1 points are

$$\xi_+(\boldsymbol{M}_1 + \delta\boldsymbol{k}) = \frac{1}{\sqrt{2}}\left(1, -e^{-i\frac{\sqrt{3}\mathfrak{a}}{2\pi}\delta k_x}\right), \tag{8}$$

$$\xi_-(-\boldsymbol{M}_1 + \delta\boldsymbol{k}) = \frac{1}{\sqrt{2}}\left(1, e^{i\frac{\sqrt{3}\mathfrak{a}}{2\pi}\delta k_x}\right) \tag{9}$$

for small deviations of $\delta\boldsymbol{k} = (\delta k_x, \delta k_y)$ from $\pm \boldsymbol{M}_1$. The periodic potential, Eqs. (7), leads to scattering between the states, $\xi_\pm$, as their momenta differ by $\boldsymbol{Q}_1$. In momentum space, the term which connects these points is $V_1 \psi^\dagger(\boldsymbol{k})\, \psi(\boldsymbol{k} + \boldsymbol{Q}_1)$. Since the unperturbed eigenspinors of Dirac CFs at $\pm\boldsymbol{M}_1$ form a Kramers pair, the scattering matrix element between them vanishes. In the vicinity of the M_1 point, the scattering matrix element depends linearly on $\delta\boldsymbol{k}$ as

$$V_1\, \xi_+^\dagger(\delta\boldsymbol{k})\, \xi_-(\delta\boldsymbol{k}) = i\frac{\sqrt{3}\, V_1 \mathfrak{a}}{2\pi}\, \delta k_x. \tag{10}$$

The CF dispersion near the M_1 point is reconstructed due to scattering off of the periodic potential. If we express a generic spinor $\chi_1(\delta\boldsymbol{k})$ near M_1 in the basis of $v_\pm = (\xi_+ \pm \xi_-)/\sqrt{2}$, we

find a Dirac Hamiltonian,

$$\mathcal{H}_1 = \delta k_y \, \chi_1^\dagger \tau^x \chi_1 + \frac{\sqrt{3}V_1 \mathfrak{a}}{2\pi} \delta k_x \, \chi_1^\dagger \tau^y \chi_1 + \cdots, \qquad (11)$$

where $\tau^{x,y,z}$ are the Pauli matrices in the $v_\pm$ basis. The corresponding results for the Dirac cones near the M_2 and M_3 points can be obtained using this result by acting with C_3 rotations. Notice that the band velocity is anisotropic and thus changes by a C_3 rotation between each M point.

Our mean-field result can be substantiated by general considerations based on symmetry (further discussion can be found in Appendix C). Because the mean-field Hamiltonian involves a single flavor of Dirac CF protected by $\mathcal{T}_{\mathrm{CF}}$ symmetry with $\mathcal{T}_{\mathrm{CF}}^2 = -\mathcal{I}$, the CF energy spectrum should be gapless and the total number of degenerate Dirac cones must be odd (as in the ordinary case of TI surface states in the presence of time reversal symmetry). By Kramers theorem, the existence of a Dirac point at momentum $\boldsymbol{k}$ implies the presence of a degenerate state at $-\boldsymbol{k}$. This leads to fermion doubling unless the Dirac cone appears *only* at BZ points that are left invariant under $\mathcal{T}_{\mathrm{CF}}$, i.e., points satisfying $\boldsymbol{k} = -\boldsymbol{k}$ mod $\boldsymbol{Q}_n$. For the triangular lattice, such points of the BZ are the Γ point and the three M points. In particular, the C_3 symmetry relating the M points implies that Dirac cones at the M points must all be degenerate. It is thus natural for the Dirac CF system discussed here to form three Dirac cones at the M points.

Introducing gauge fluctuations to the mean-field result, Eq. (11), one obtains at $f = 1$ three Dirac fermions coupled to the U(1) gauge field, a_μ. The band velocities of these Dirac fermions are anisotropic, each differing by a C_3 rotation. However, the large-N_f QED$_3$ fixed point is stable to both velocity anisotropy and differences in the velocity of each Dirac species [62]. We therefore reasonably expect that the long wavelength theory has emergent Lorentz invariance, and each χ_I fermion has the same velocity $v \equiv 1$. Hence, $N_f = 3$ QED$_3$ arises as an effective theory at length scales much greater than the period of the oscillatory magnetic field $\mathfrak{a}$,

$$S_{\mathrm{eff}} = \int_{t,\boldsymbol{x}} \left[\sum_{I=1}^{3} i \bar{\chi}_I (\partial_\mu - i a_\mu) \gamma^\mu \chi_I + \frac{1}{4\pi} A' da \right], \qquad (12)$$

where again $\gamma^\mu = (\tau^z, i\tau^x, i\tau^y)$, and we define $A' \equiv A_{\mathrm{total}} - A$ to be a background probe field on top of the original background field, A_μ, that produces $B(\boldsymbol{x})$. We omit the Maxwell term for a, which is irrelevant in the renormalization group sense (but is necessary as a UV regulator). Notice that what started as a discrete C_3 symmetry in the UV has been enhanced to an emergent SU(3) flavor symmetry, $\chi_I \to U_{IJ}\chi_J$, at low energies.[2] See Appendices C and D for a discussion of how discrete symmetries such as parity and time-reversal act in the effective $N_f = 3$ QED$_3$ theory.

Furthermore, our mean-field arguments do not depend on the detailed choice of density-density interaction potential, $V_{\mathrm{int}}(\rho_e)$, for the Dirac electrons, which simply maps to a flux-flux interaction, $V_{\mathrm{int}}(b_*)$, in the dual theory. In particular, we

note that instantaneous Coulomb interactions are expected to be marginally irrelevant at the QED$_3$ fixed point [64], while a Lorentz invariant generalization of Coulomb interactions is exactly marginal and leads to a line of fixed points with self-dual properties [51,53,65,66].

IV. QED$_3$ AS A FCI PLATEAU TRANSITION

In ordinary quantum Hall systems, incompressible FQH phases are achieved when the filling is tuned away from the CFL state at $\nu = 1/2$, with Hall conductivity set by the filling. In striking contrast, here we show that incompressible states with fractional Hall conductivity, known as FCI states, can be induced *fixed at half-filling* for the electronic Chern band by introducing a periodic chemical potential.

Our QED$_3$ state is protected by the electronic $\mathcal{PH}$ symmetry. When $\mathcal{PH}$ is broken, this critical state can become unstable and transition into a new state. By introducing a periodic electrostatic potential to break $\mathcal{PH}$, we find the QED$_3$ state gives way to FCI phases, while maintaining half filling of the electronic Chern band. We consider a potential that is commensurate with the vortex lattice,

$$V_e(\boldsymbol{x}) = 2\mu_1 \sum_{n=1}^{6} \cos(\boldsymbol{Q}_n \cdot \boldsymbol{x}), \qquad (13)$$

which has zero spatial mean. It generates the singlet mass operator, $m\Delta_{\mathrm{singlet}} = m \sum_I \bar{\chi}_I \chi_I$, with $\mathrm{sgn}(m) = \mathrm{sgn}(\mu_1)$.

From the fermion-vortex duality, Eqs. (3), we see that $V_e(\boldsymbol{x})$ sources a periodic magnetic field felt by the CFs, $\bar{b}_*(\boldsymbol{x})$, which we choose to write in terms of a vector potential, $\bar{a}_i(\boldsymbol{x}) = \varepsilon_{ij}\partial_j \bar{\phi}(\boldsymbol{x})$, where $\bar{\phi}(\boldsymbol{x})$ is a bounded, real-valued function with the same periodicity as $\bar{a}$. We find numerically in the lower panel of Fig. 3 that the combination of periodic potential and periodic gauge field opens a gap in the mean-field CF dispersion. In other words, the emergent Dirac fermion in our QED$_3$ state now acquires a finite mass.

The origin of gap opening can also be understood by a perturbative analysis. We proceed analogously to the arguments leading to Eq. (11). For momenta near $\boldsymbol{M}_1$, the relevant scattering process induced by the periodic gauge field has wave vectors $\boldsymbol{Q}_1, \boldsymbol{Q}_4 = -\boldsymbol{Q}_1$. Denoting the amplitude of $\bar{\phi}(\boldsymbol{x})$ by Φ and using the matrix element $\xi_+(0)\gamma^t\gamma^x\xi_-(0) = i$, we find that the mean-field Hamiltonian contains a Dirac mass term,

$$\mathcal{H}_1' = \bar{a}_x(\boldsymbol{Q}_1) \, \psi^\dagger(\boldsymbol{M}_1) \gamma^x \psi(-\boldsymbol{M}_1) + \mathrm{H.c.} \qquad (14)$$

$$\propto \frac{\pi \Phi}{\mathfrak{a}} \chi_1^\dagger \tau^z \chi_1, \qquad (15)$$

where χ_1 was defined above Eq. (11) and $\mathrm{sgn}(\Phi) = \mathrm{sgn}(\mu_1)$. The analogous calculation can be readily performed for the other two species, yielding a mass, $m \sum_I \bar{\chi}_I \chi_I$, $\mathrm{sgn}(m) = \mathrm{sgn}(\mu_1)$.

When the χ_I fermions become massive, one obtains a CF Chern insulator with Chern number $3\,\mathrm{sgn}(m)/2$. Integrating out the fermions and gauge fluctuations, we see that the periodic scalar potential in Eq. (13) tunes an FCI transition across which the Hall conductivity changes by

$$\Delta \sigma_{xy} = \frac{1}{3}\frac{e^2}{h}, \qquad (16)$$

---

[2]There is a possibility the theory in Eq. (12) may be unstable to dynamical mass generation, leading to a trivial state with finite correlation length. See the discussion in Ref. [63] for a review.

with the two topological orders on each side of the transition corresponding to the $\nu = \pm 1/3$ Laughlin states (see Appendix E).

It is also of interest to consider scalar potentials that break the C_6 lattice symmetry by having different amplitudes, $\mu_1^{(n)}$, for each $\boldsymbol{Q}_n$ vector. Such deformations generically introduce an octet of mass operators of the form $\Delta_{\text{octet}}^b = \sum_{I,J} \bar{\chi}_I t_{IJ}^b \chi_J$, where t^b, $b = 1, \ldots, 8$, are the generators of SU(3). These operators can tune the theory to (1) the FCI states described above, as well as (2) a Chern insulator state with integer Hall response occurring when one of the χ_I fermions receives a mass with opposite sign from the other two, and, finally, (3) a $\mathcal{PH}$-preserving state where one of the emergent Dirac fermions is gapless and the remaining two are gapped with opposite sign.

V. DOPING QED$_3$: FCI JAIN SEQUENCE

We now consider finite doping from charge neutrality—which breaks the electronic $\mathcal{PH}$—and varying B_0 away from the case of two flux per unit cell. We find that our emergent QED$_3$ theory gives way to a family of FCI states, in analogy with how the CFL is a parent state for the celebrated Jain sequence of observed Abelian FQH phases. At finite doping ρ_e, the χ_I fermions feel a uniform emergent magnetic field, b_*, and form their own LLs (including the zeroth LL). When an integer number of these LLs are completely filled, an incompressible FCI appears. This occurs when the χ_I fermions are at filling:

$$\nu_\chi = 2\pi \sum_I \frac{\langle \chi_I^\dagger \chi_I \rangle}{b_*} = 3 \left(q - \frac{1}{2} \right), \quad q \in \mathbb{Z}. \tag{17}$$

Here the $1/2$ term comes from the zeroth LL of the emergent Dirac fermions in our QED$_3$ state, and the factor of 3 accounts for the three flavors. From Eq. (12), we observe that the emergent Dirac fermion density is set by the deviation from B_0, denoted $B' = \varepsilon_{ij} \partial_i A'_j = -(4\pi) \sum_I \chi_I^\dagger \chi_I$, and that the background charge density leads to an emergent magnetic field, $\rho_e = b_*/4\pi$. Combining these relations with Eq. (17), we see by the Streda formula that the resulting incompressible FCI phase has Hall conductivity:

$$\sigma_{xy} = 2\pi \frac{d\rho_e}{dB'} = -\frac{1}{12q - 6} \frac{e^2}{h}. \tag{18}$$

Here σ_{xy} is the Hall conductivity associated with a single TI surface, of which the contribution from the half-filled Chern band is $\sigma_{xy}^0 = \sigma_{xy} + 1/2$ in units of e^2/h (because Chern bands at negative energies contribute $-1/2$). Comparing $\sigma_{xy}^0 = (3q - 2)/(6q - 3)$ with the Jain sequence, $\sigma_{xy}^{\text{Jain}} = p/(2p+1)$, we find that each of these fractions lies on the principal Jain sequence and has the same topological order as their associated Jain states. Importantly, only the Jain sequence states satisfying $p = 3q - 2$ appear on the FCI sequence in Eq. (18). One therefore expects to measure a Landau fan of FCI states in a Chern band near half filling, with slopes given by Eq. (18), as shown in Fig. 4.
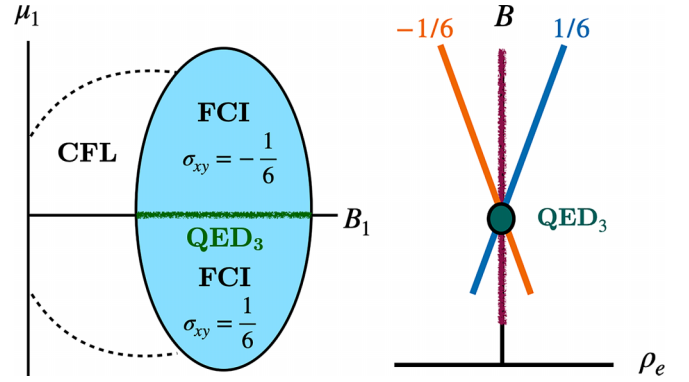
FIG. 4. Two ways to access FCI phases. Left: By tuning a periodic scalar potential with strength μ_1 while remaining fixed at half filling, the emergent Dirac fermions become massive, leading to FCI states. Note that in this figure, the Hall conductivity is that which would be measured on a single TI surface. Right: By doping away from $N_f = 3$ QED$_3$ with a uniform electron density, ρ_e, and magnetic field $B' = B - B_0$. In this case, the emergent $N_f = 3$ QED$_3$ phase gives way to a sequence of incompressible FCI states. The magenta segment on the B axis denotes the CFL phase. The green dot corresponds to the case of two flux quanta per unit cell, where the quantum critical QED$_3$ phase appears.

VI. UNIVERSAL PROPERTIES OF THE EMERGENT QED$_3$ STATE

The quantum critical $N_f = 3$ QED$_3$ phase is characterized by a range of universal observable properties which contrast the uniform CFL metal occurring in the absence of a periodic magnetic field, $B_1 = 0$. In this section, we describe several of the most prominent such properties.

Among the most basic universal properties of the $N_f = 3$ QED$_3$ theory in Eq. (12) are the scaling dimensions of the mass operators, denoted $[\Delta_{\text{singlet}}]$ and $[\Delta_{\text{octet}}]$, which determine the divergence of the correlation length as the transition is crossed. For example, tuning the FCI transition with a periodic scalar potential will lead to a diverging correlation length exponent, $\xi \sim (\mu_1)^{-\nu}$, with $\nu = 1/(3 - [\Delta_{\text{singlet}}])$. The values of $[\Delta_{\text{singlet}}]$ and $[\Delta_{\text{octet}}]$ can be calculated in the large-N_f expansion [62,67–69], but the validity of extending these results to small N_f is unclear. Were one to establish an experimental or numerical realization of our setup, it could be possible to measure these exponents, either directly from the correlation functions of the mass operators in numerics or by measuring the scaling of the DC conductivity, $\sigma_{xx} \sim f(\omega/T, \mu_1/T^{\nu z})$ with $z = 1$ [70].

The DC conductivity of quantum critical states in 2D is another essential piece of universal data. Because the EM current of the theory in Eq. (12) is the emergent electric field, $J_i = \varepsilon_{ij} e_j/4\pi$, $e_i = \partial_i a_t - \partial_t a_i$, one obtains for a rotationally invariant system,

$$\sigma\left(\frac{\omega}{T}\right) = \frac{i\omega}{(4\pi)^2} \Pi^{-1}\left(\frac{\omega}{T}\right), \tag{19}$$

where $\Pi_{xx} = \Pi_{yy} \equiv \Pi$ is the polarization of the emergent gauge field. Both the DC ($\omega/T \to 0$) and optical ($T/\omega \to 0$) conductivities are universal numbers of $O(e^2/h)$, but they do not necessarily take the same value [71]. This is in contrast to the Dirac CFL metal at $B_1 = 0$, where the DC conductivity

should be set by disorder and is much smaller than e^2/h in sufficiently clean systems [20].

The universal conductivity of QED$_3$ can again be calculated in the large-N_f limit, which gives [72]

$$\sigma\left(\frac{\omega}{T} \to 0\right) \to \infty, \quad \sigma\left(\frac{T}{\omega} \to 0\right) = \frac{2}{\pi N_f}\frac{e^2}{h}, \quad (20)$$

suggesting that in the clean limit the theory may be a perfect conductor with diverging DC conductivity and vanishing density of states. Note that to obtain this result, one computes *the resistivity* in the large-N_f limit, using $\Pi(\omega, \boldsymbol{q} = 0) = iN_f\omega(\frac{1}{16} + O(N_f^{-1}))$ (for $T = 0$), and then inverts the result to obtain the conductivity. This is why the leading contribution to the conductivity goes as $1/N_f$.

Similarly, the electronic compressibility is given by the correlator of the emergent magnetic field, since $\rho_e = b_*/4\pi$. Because of the scale invariance of $N_f = 3$ QED$_3$, the static compressibility should vanish linearly as $T \to 0$, $\kappa(T) \sim T$. This is in contrast to the CFL phase, which has finite compressibility as $T \to 0$. Additionally, the heat capacity of QED$_3$ at large N_f has the form $C \sim T^{2+\eta}$, $\eta \sim O(1/N_f)$, whereas for the CFL metal the heat capacity should, in general, exhibit a distinct power law, e.g., $C \sim T^{2/3}$ in systems with short-ranged interactions and $C \sim T \log T$ for systems with long-ranged $1/r$ Coulomb interactions.

We finally comment that truly realistic systems have quenched disorder, which will cause QED$_3$ theories to run to a new fixed point governed by an interplay of disorder and interactions [64,72–75]. In the $N_f = 3$ theory, $\mathcal{PH}$-symmetric disorder (a random magnetic field component for the electrons) is exactly marginal, leading to a line of fixed points with varying dynamical critical exponent, $z > 1$. For generic disorder breaking $\mathcal{PH}$, the theory runs to strong disorder and gives way to diffusion ($z = 2$), leading to a quantum critical point governed by a gauged nonlinear sigma model (NLSM) [76,77], which at mean-field level resembles Pruisken's theory of the IQH transition [78,79]. Determining the universal properties of NLSMs of this type remains an important open problem.

VII. DISCUSSION

Starting with a TI surface in a periodic magnetic field, we have demonstrated that half-filled LLs of Dirac electrons in spatially periodic magnetic fields can give rise to exotic quantum critical states—namely, $N_f = 3$ QED$_3$—without any fine-tuning. This critical state is protected by the particle-hole symmetry of the Dirac electrons at charge neutrality.

Although exact particle-hole symmetry is necessary to reach the quantum critical QED$_3$ state without fine-tuning, realistic TI films break particle-hole symmetry at finite field due to the presence of a nonvanishing Zeeman term. One may therefore naturally expect that this term gaps the emergent Dirac cones and results in the appearance of a gapped state, as opposed to a quantum critical phase. However, if the breaking of particle-hole symmetry is weak, this gap may be quite small, and thus the physics of the quantum critical QED$_3$ phase may still be accessible with fine-tuning of external fields. We leave the detailed development of material realizations to future work.

Our paper establishes possibilities for strongly correlated gapless states at half filling of Chern bands that may be applicable in even further contexts. Indeed, an emergent particle-hole symmetry may be found in the growing landscape of Chern band systems at half filling, as occurs in the case in half-filled LLs at high magnetic fields. Thus, the exotic quantum critical physics described in this paper may be a more general feature of half-filled Chern bands. Speaking more broadly, half-filled Chern bands provide ample opportunities for realizing unique quantum states of matter and call for much further study.

APPENDIX A: MEAN FIELD CF BAND STRUCTURE

Here we describe the numerical calculation of the mean-field CF band structure in the presence of a periodic modulation, Eq. (6). A more complete depiction of the band
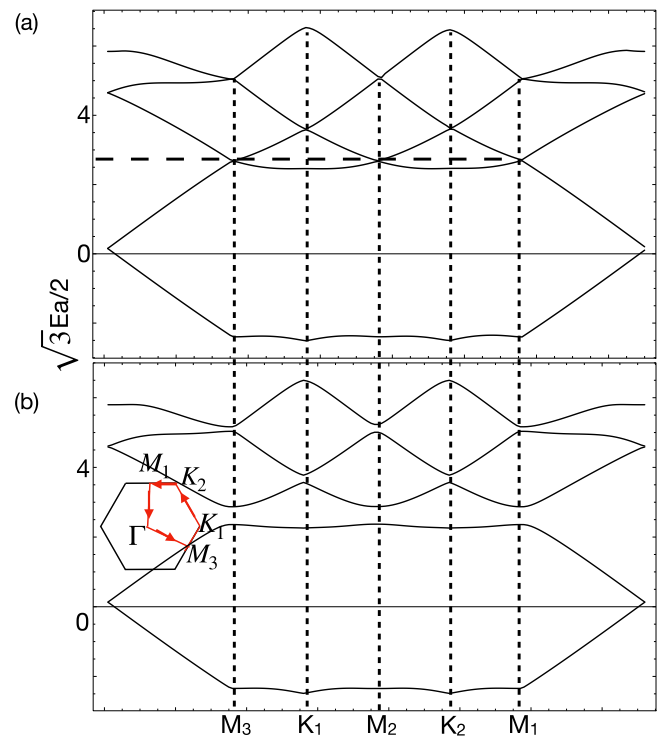
FIG. 5. The dispersion of the CFs under a periodic potential, Eqs. (7), with $V_1 = 2/(\sqrt{3}\mathfrak{a})$ showing more bands and Dirac fermions at M, K points. Physical settings are identical to main text Fig. 3.
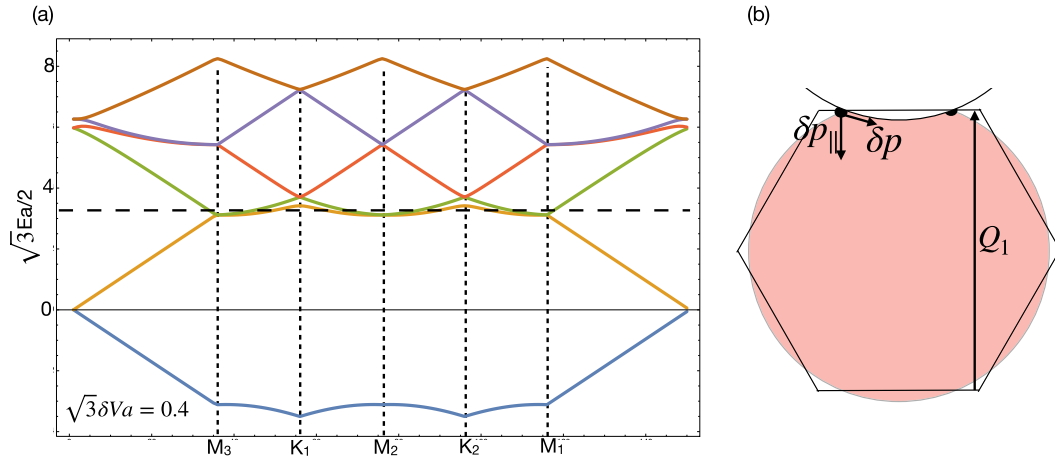
FIG. 6. (a) The dispersion of CFs under exact diagonalization when B_1 is small compared with B_0. The dashed line indicates Fermi energy that crosses bands, creating CF particle and hole pockets plotted in Fig. 2(a). (b) An illustration of the integration in Eq. (B8) near a particular intersection point between circular Fermi surface and the Brillouin zone. The red shade denotes momenta $\boldsymbol{p}$'s which scatter to $p - Q_1$ and give nonzero contribution to the integral.

structure is provided in Fig. 5. After mapping to the Dirac CF picture, one has a Dirac cone lying at the Γ point below the Fermi energy. As described in the main text, the periodic magnetic field can be viewed as a periodic CF chemical potential. Thus, at leading order, the periodic magnetic field scatters the CFs with a momentum difference of the reciprocal super-lattice vectors, $\boldsymbol{Q}_n$. In momentum space, the single-particle Hamiltonian is

$$\mathcal{H}_{\text{CF}} = \int d^2\boldsymbol{p}\, \bar{\psi}(\boldsymbol{p})\,(\gamma^i p_i)\,\psi(\boldsymbol{p}) + V_1 \sum_{n=1}^{6} \psi^\dagger(\boldsymbol{p})\psi(\boldsymbol{p} + \boldsymbol{Q}_n).$$

(A1)

For a particular $\boldsymbol{p}$ in the first BZ, the scattering process involves states with momenta $\boldsymbol{p}, \boldsymbol{p} + \boldsymbol{Q}_n, \boldsymbol{p} + 2\boldsymbol{Q}_n \cdots$ and we take the momentum cutoff to $\boldsymbol{p} + 3\boldsymbol{Q}_n$ for the numerical diagonalization. Figure 6(a) shows a dispersion for small B_1 which for CFs deforms the circular Fermi surface into particle/hole pockets.

When solving for the mean field of CFs under an internal magnetic field b^* from chemical potential modulation on physical electrons, we take

$$\bar{a}_i = \epsilon^{ij}\partial_j \phi(\boldsymbol{x}), \quad \phi(\boldsymbol{x}) = \phi_0 \sum_{n=1}^{6} \cos(\boldsymbol{Q}_n \cdot \boldsymbol{x}).$$

(A2)

The vector potential $\bar{a}$ thus has nontrivial Fourier component at reciprocal lattice vectors $\bar{a}_i(Q_k) = i\epsilon^{ij}Q_{k,j}\phi_0$ where $k = 1 \cdots 6$, $i, j = x, y$. This connects CF states with the momentum difference of Q_k, i.e., resulting in additional terms:

$$\mathcal{H}_a = \sum_{n=1}^{6} \bar{a}_i(Q_k)\bar{\psi}_{\boldsymbol{p}}\gamma^i\psi_{\boldsymbol{p}+\boldsymbol{Q}_n}.$$

(A3)

APPENDIX B: PERIODIC POTENTIAL OF CFS FROM PERIODIC MAGNETIC FIELD OF PHYSICAL ELECTRONS

To perform our mean-field analysis, it was necessary to pass to a CF description with fixed chemical potential rather than fixed density (i.e., pass from the canonical to the grand canonical ensemble). Here we describe how to calculate the profile of the needed CF chemical potential, $V_{\text{CF}}(\boldsymbol{x})$ in Eqs. (7), induced by a periodic modulation in the magnetic field. From dimensional analysis, it is natural to guess the leading behavior,

$$|V_1| \sim \frac{|B_1|}{\sqrt{|B_0|}} + \cdots,$$

(B1)

where V_1 is defined in Eqs. (7) as the amplitude of the oscillating part of the CF chemical potential:

$$V_{\text{CF}}(\boldsymbol{x}) = \mu_0 + V_1 \sum_{n=1,\ldots,6} e^{i\boldsymbol{Q}_n\cdot\boldsymbol{x}}.$$

(B2)

Indeed, Eq. (B1) makes physical sense—the quantity has dimensions of energy and vanishes as $B_1 \to 0$ (the periodic potential turns off) or $B_0 \to \infty$ (the periodic modulation is small on the scale of the Fermi wave vector).

The proportionality coefficient in Eq. (B1) can be determined by enforcing self-consistently,

$$\langle \psi^\dagger\psi(\boldsymbol{x})\rangle_{V_{\text{CF}}(\boldsymbol{x})} = \frac{B(\boldsymbol{x})}{4\pi},$$

(B3)

working power by power in B_1/B_0. Although this perturbative approximation may not hold for the situation of physical interest, $|B_0| \sim |B_1|$, we expect it to give a reasonable estimate for the relationship between B_1 and V_1 (we emphasize that the spatial periods of V_1 and B_1 are identical, independent of any perturbative approximation). Wick rotating to imaginary time, $t = -i\tau$, we single out the $\boldsymbol{Q}_n$ Fourier components of

the density one-point function,

$$\langle \psi^\dagger \psi(\boldsymbol{Q}_n) \rangle = \frac{1}{2\pi} \int d^2\boldsymbol{x} \, \text{Tr}[G_{\psi^\dagger\psi}(\boldsymbol{x}, \boldsymbol{x}, \tau \to 0)] e^{i\boldsymbol{Q}_n\boldsymbol{x}}$$

$$= \frac{B(\boldsymbol{Q}_n)}{4\pi},$$

$$G_{\psi^\dagger\psi}(\boldsymbol{x}, \boldsymbol{x}, i\omega) = (i\omega + i\gamma_0\gamma^i\partial_i + V_{\text{CF}}(\boldsymbol{x}))^{-1}. \quad (B4)$$

In the regime where $|V_1| \ll |\mu_0|$, i.e., $B_1 \ll B_0$, we can expand Eq. (B4) with a small parameter $\frac{V_1}{\mu_0}$:

$$G_{\psi^\dagger\psi}(\boldsymbol{x}, i\omega) = G_0 + \delta G = G_0 - G_0(V_{\text{CF}}(\boldsymbol{x}) - \mu_0)G_0 + \cdots,$$

$$G_0 = (i\omega + i\gamma_0\gamma^i\partial_i + \mu_0)^{-1}. \quad (B5)$$

Keeping only the leading (one-loop) contribution, we obtain for the oscillating part, δG:

$$\delta G = -\int d^2\boldsymbol{p}\, d\omega \, \text{Tr}[G_0(\boldsymbol{p}, i\omega) V_1 G_0(\boldsymbol{p} + \boldsymbol{Q}_n, i\omega)] = \frac{B_1(\boldsymbol{Q}_n)}{4\pi}. \quad (B6)$$

We find it convenient to express the Green's function in the eigenenergy basis for each momentum $\boldsymbol{p}$, rewriting $G_0(\boldsymbol{p}, i\omega) = P(\boldsymbol{p})(i\omega + |p| + \mu_0)^{-1} + (1 - P(\boldsymbol{p}))(i\omega - |p| + \mu_0)^{-1}$ in terms of the projection operator, $P(\boldsymbol{p})$, that projects the Dirac spinor onto the positive energy band. The frequency integral has the general form

$$\int d\omega \, (i\omega + \epsilon_1)^{-1}(i\omega + \epsilon_2)^{-1} = 1 - \Theta(-\epsilon_1\epsilon_2)\frac{1}{|\epsilon_1 - \epsilon_2|}. \quad (B7)$$

Here $\Theta(X)$ is the Heaviside step function, which tells us that the negative energy states (well below the chemical potential) do not contribute. Furthermore, for states with positive energy, we observe that only when $\boldsymbol{p}$ and $p + \boldsymbol{Q}_n$ are above and below the Fermi surface will the integral in Eq. (B6) be nonzero. The dominant contribution comes when the energies at momenta $\boldsymbol{p}, \boldsymbol{p} + \boldsymbol{Q}_n$ are close. For the specific $\boldsymbol{Q}_n$ for the hexagonal BZ, one concludes that the integral is most singular at the momenta where the original circular Fermi surface (for integer filling, i.e., with the same area as the first BZ) intersects the hexagonal BZ. Linearizing the deviation from one intersection point as $\delta\boldsymbol{p}$, we have for the integral in Eq. (B6) [see Fig. 6(b)]

$$\int d(\delta p)\, d(\delta p_\parallel) \frac{\xi_{\boldsymbol{p}, \boldsymbol{p} + \boldsymbol{Q}_n}}{v_\perp \delta p + v_\parallel \delta p_\parallel} V_1 = \frac{B_1(\boldsymbol{Q}_n)}{4\pi}, \quad (B8)$$

where $\xi_{\boldsymbol{p}, \boldsymbol{p} + \boldsymbol{Q}_n} = \text{Tr}[P(p)P(p + \boldsymbol{Q}_n)]$ and $\delta p_\parallel$ is the momentum projected along $\boldsymbol{Q}_n$ (not to be confused with the momentum along the Fermi surface). The above integral is regular and can be calculated numerically. However, since the regime of interest corresponds to the case $B_1/B_0, V_1/V_0 \sim O(1)$, we do not expect the final coefficient, $C \sim O(1)$ to be physically meaningful. We therefore confirm the expectation from dimensional analysis and estimate

$$C\sqrt{B_0} V_1 = \frac{B_1(\boldsymbol{Q}_n)}{4\pi}, \quad (B9)$$

where the factor $\sqrt{B_0}$ comes in from the $|\boldsymbol{Q}_n|$ dependence on the unit cell size and hence B_0, given that unit cell

size S satisfies $B_0 S = 4\pi$. We have $|\boldsymbol{Q}_n| \propto \sqrt{B_0}$ and the expression Eq. (B8) scales as $|\boldsymbol{Q}_n| \sim \sqrt{B_0}$. The above conclusion should be modified quantitatively in the regime where $B_1 \sim B_0$ that QED_3 emerges, where one does not have a controlled way for calculation. The scaling and relation between V_1, B_1 remain true in this regime due to dimensional analysis.

APPENDIX C: POSITION OF THE EMERGENT CF DIRAC CONES

We show that the emergent Dirac cones for CFs are pinned at certain high-symmetry points—including $M_i, K(K')$ at the BZ edge and Γ at the BZ center.

Two threads of arguments are presented: From the anomaly of the CFs, i.e., parity anomaly in $\mathcal{PH} \rtimes U(1)_\psi$, at mean-field level for a fixed energy, the spectrum has to be either gapless or possess an odd number of Dirac cones to match the anomaly. For the Dirac cone case, note that $\mathcal{PH}$ sends momenta $k \to -k$ due to its antiunitary action. Hence, generically, the Dirac cones come in pairs, except at high-symmetry point M_i's since $\pm M_i$ differ by a reciprocal lattice vector and one could have an odd number of Dirac cones pinned at M_i's. Another possibility is a single Dirac cone at Γ, which is $\mathcal{PH}$ invariant. For filling 1 for CFs focused in the main text, we have the case for Dirac cones emerging at M_i's.

Another argument follows from symmetry of the CF action: $\mathcal{PH}$ leaves M_i, Γ's invariant and squares to -1. Hence there is a Kramers degeneracy at M_i, Γ's.

To see the appearance of Dirac cones at $K, \tilde{K} = -K$ points, which in our case occurs between the second and third Bloch bands in energy (along with the Dirac cone at Γ to cancel the parity anomaly), we consider two relevant symmetries $C_3, \mathcal{PH} \cdot \mathcal{P}$, with the action on the CFs

$$C_3 : \psi(r) \to e^{-i\sigma^z\frac{\pi}{3}}\psi(C_3(r)),$$

$$\mathcal{PH} \cdot \mathcal{P} : \psi \to \sigma^z\psi. \quad (C1)$$

We show that acting on the eigenstates with momenta K and its C_3 equivalents K', K'', the two symmetries do not commute, which implies degeneracy. The Bloch wave functions with positive energy for the CFL action Eq. (2) are taken to be

$$\psi_K : (1, e^{i\theta})^T, \psi_{K'} : C_3(\psi_K) = (e^{-2i\theta}, e^{i3\theta})^T,$$

$$\psi_{K''} : -C_3^{-1}(\psi_K) = (e^{-4i\theta}, e^{i5\theta})^T. \quad (C2)$$

Under such basis, the transformation matrix for $C_3, \mathcal{PH} \cdot \mathcal{P}$ reads

$$C_3 : \begin{pmatrix} 0 & 1 & 0 \\ 0 & 0 & 1 \\ 1 & 0 & 0 \end{pmatrix},$$

$$\mathcal{PH} \cdot \mathcal{P} : \begin{pmatrix} 0 & e^{2i\theta} & 0 \\ e^{2i\theta} & 0 & 0 \\ 0 & 0 & -e^{2i\theta} \end{pmatrix}. \quad (C3)$$

which do not commute. Hence the degeneracy at $K, \tilde{K} = -K$ are enforced.

APPENDIX D: SYMMETRY ACTION ON THE EMERGENT DIRAC CONES

Here we specify how different symmetries act on the emergent Dirac fermions, χ_I, $I = 1, 2, 3$, of the emergent QED$_3$ theory. We start with the lattice translations and C_3 rotations,

$$
\begin{aligned}
T_i &: \chi_I \to e^{i\boldsymbol{M}_I \cdot \boldsymbol{x}} \chi_I, \\
C_3 &: \chi_I \to e^{i\gamma' \frac{\pi}{3}} \chi_{(I+1)\bmod 3}.
\end{aligned}
\tag{D1}
$$

Here $\boldsymbol{M}_I$ are the reciprocal lattice vectors corresponding to the three M points. As described in the main text, at long wavelengths the C_3 rotation symmetry is enhanced to an emergent SU(3) flavor symmetry.

The discrete symmetries of most interest to us are the antiunitary (electronic) particle-hole and parity symmetries, which we denote $\mathcal{CT}$ (the product of charge conjugation and time-reversal) and $\mathcal{CP}$,

$$
\begin{aligned}
\mathcal{CT} &: \chi_I \to -i\tau^y \chi_I(-t, \boldsymbol{x}), & (a_0, a_i) &\to (a_0, -a_i) \\
\mathcal{CP} &: \chi_I \to \tau^x \chi_{s(I)}(t, -x, y), & (a_0, a_i) &\to (a_0, -a_x, a_y),
\end{aligned}
\tag{D2}
$$

where $s(I)$ permutes the Dirac fermion species as $s(1) = 1$, $s(I = 2, 3) = 5 - I$. The emergent $N_f = 3$ QED$_3$ theory is invariant under these symmetries. Both are broken by the introduction of a periodic scalar potential, i.e., the Dirac mass operator.

APPENDIX E: TOPOLOGICAL ORDERS OF THE FCI STATES

Here we consider the topological orders of the FCI states considered in the main text. This requires introducing an auxiliary gauge field, b_μ, to the $N_f = 3$ QED$_3$ theory such that all Chern-Simons terms are properly quantized and the theory is gauge invariant:

$$
\begin{aligned}
S = \int_{t,\boldsymbol{x}} \sum_{I=1}^{3} i\bar{\chi}_I (\partial_\mu - ia_\mu)\gamma^\mu \chi_I - \frac{1}{8\pi} ada - \frac{2}{4\pi} bdb \\
+ \frac{1}{2\pi} bd(a + A') - \frac{1}{8\pi} A'dA'.
\end{aligned}
\tag{E1}
$$

Note here that a_μ is a spin$_c$ connection, while b_μ is an ordinary U(1) connection. See, e.g., Refs. [49,80] for a more detailed discussion of the difference between spin$_c$ and U(1) connections. For our needs, the only important consequence of this distinction is that anyons associated with a_μ will have their statistics shifted by π, since spin$_c$ connections couple to fermions. Note also that we continue to consider the theory on the surface of a TI, the bulk of which gives rise to the final $A'dA'/8\pi$ term.

One can easily recover the action discussed in the main text, Eq. (12), by integrating out b_μ, meaning that the local physics of the two theories is equivalent. However, unlike Eq. (12), this theory is gauge invariant on any manifold. This is crucial for correctly diagnosing the topological order on integrating out the χ_I fields deep in a FCI phase.

We begin by considering the effect of a singlet mass term, $\mathcal{L}_{\text{mass}} = -m \sum_I \bar{\chi}_I \chi_I$, which is generated by the periodic scalar potential in Eq. (13). This deformation causes the χ_I fermions to form Chern insulators, each with Chern number $\operatorname{sgn}(m)/2$. The resulting state is a FCI described by the topological quantum field theory (TQFT) with Lagrangian

$$
\begin{aligned}
\mathcal{L}_{\text{FCI}} = \frac{3\operatorname{sgn}(m) - 1}{2} \frac{1}{4\pi} ada - \frac{2}{4\pi} bdb \\
+ \frac{1}{2\pi} bd(a + A') - \frac{1}{8\pi} A'dA'.
\end{aligned}
\tag{E2}
$$

The Hall conductivity of this state can be calculated by integrating out both gauge fields,

$$
\mathcal{L}_{\text{response}} = \left(\frac{1}{2} - \frac{\operatorname{sgn}(m)}{6} \right) \frac{1}{4\pi} A'dA' - \frac{1}{8\pi} A'dA',
\tag{E3}
$$

where we have separated out the bulk TI contribution. Indeed, the first term has coefficient $1/3$ ($m > 0$) or $2/3$ ($m < 0$), suggesting that these states have the topological order of the $\nu = \pm 1/3$ Laughlin states. We can furthermore calculate the ground-state degeneracy on the torus, which is $|\det K| = 3$, where K is the $(3\operatorname{sgn}(m)/2 - 1/2, -2, 1)$ K matrix corresponding to Eq. (E2), in agreement with this expectation.

The equivalence can be established more concretely at the level of the TQFT. We start with the case $m > 0$. In this case, the first term in Eq. (E2) is a trivial TQFT, $ada/4\pi$. Indeed, in this case we can integrate out a in a gauge invariant way to obtain

$$
\mathcal{L}_{m>0} = -\frac{3}{4\pi} bdb + \frac{1}{2\pi} bdA' - \frac{1}{8\pi} A'dA'.
\tag{E4}
$$

This is of course the usual Laughlin U(1)$_{-3}$ state, with the same charge-$1/3$ anyonic quasiparticles as the usual Laughlin FQH state. Notice that the fluctuating gauge field here is an ordinary U(1) connection, as the spin$_c$ connection has been eliminated.

We now consider the case of $m < 0$. Here we cannot immediately integrate out a_μ, but we can nevertheless argue its equivalence to a Laughlin state. We start by using a trick to simplify the TQFT (which in this case incorporates the same physics as the more rigorous notion of level-rank duality; see Refs. [53,80] for an introduction accessible to condensed matter physicists). We start by introducing a background CF world line, j_f^μ, coupling to a_μ. Because j_f^μ describes a fermion, we can use flux attachment to rewrite it in terms of a bosonic world-line variable, J^μ, with a single flux attached,

$$
j_f^\mu a_\mu \to J^\mu \beta_\mu + \frac{1}{4\pi} (\beta + a)d(\beta + a),
\tag{E5}
$$

where β_μ is a new U(1) gauge field implementing the flux attachment. Its role is to explicitly implement the aforementioned shift of the anyon statistics by π associated with the fact that a_μ is a spin$_c$ connection. Therefore, rather than working with a TQFT where one probes with fermionic lines, we can equivalently work with a different representation of the TQFT where all the probes are bosonic. We therefore arrive at an equivalent TQFT,

$$
\begin{aligned}
\mathcal{L}_{m<0} = \frac{1}{4\pi} \beta d\beta + \frac{1}{2\pi} \beta da - \frac{1}{4\pi} ada - \frac{2}{4\pi} bdb \\
+ \frac{1}{2\pi} bd(a + A') - \frac{1}{8\pi} A'dA',
\end{aligned}
\tag{E6}
$$

where we have dropped the dependence on the probe, J^μ. Now again the theory involves a trivial TQFT for a_μ, and we can integrate it out in the same way as before to obtain

$$\mathcal{L}_{m<0} = \frac{2}{4\pi}\beta d\beta + \frac{1}{2\pi}bd(\beta + A') - \frac{1}{4\pi}bdb - \frac{1}{8\pi}A'dA',$$
(E7)

which, incidentally, is the TQFT we would have found had we invoked the level-rank duality between $U(1)_{-2}$ (with a spin$_c$ connection) and $U(1)_2$ (with an ordinary $U(1)$ connection). We can integrate out b_μ to obtain the properly quantized, single-component TQFT:

$$\mathcal{L}_{m<0} = \frac{3}{4\pi}\beta d\beta + \frac{1}{2\pi}\beta dA' + \frac{1}{8\pi}A'dA'.$$
(E8)

From here, one can easily confirm that this theory has the correct Hall conductivity and ground-state degeneracy. We therefore observe that the $m < 0$ state is equivalent to a $U(1)_3$ TQFT, which is the particle-hole conjugate of the $U(1)_{-3}$ state found for $m > 0$.

In the case of the FCI sequence accessed by filling $q \in \mathbb{Z}$ LLs of the χ_I fermions, the TQFT one obtains is

$$\mathcal{L}_{\text{FCI Jain}} = \frac{3q-2}{4\pi}ada - \frac{2}{4\pi}bdb$$
$$+ \frac{1}{2\pi}bd(a + A') - \frac{1}{8\pi}A'dA'.$$
(E9)

Note that the $q = 0$ and $q = 1$ states are the same as the states we found by turning on mass operators with $m < 0$ and $m > 0$, respectively. This general sequence of states have K matrices that each correspond to a state on the principal Jain sequence. Indeed, each Jain state can be described by a 2×2 K-matrix with label $(k, -2, 1)$, $k \in \mathbb{Z}$, where the gauge field with level k is a spin$_c$ connection (i.e., couples to CFs). The anyon content of each of these states can be found discussed in numerous references, e.g., Refs. [45,81].

[1] Y. Cao, V. Fatemi, S. Fang, K. Watanabe, T. Taniguchi, E. Kaxiras, and P. Jarillo-Herrero, Unconventional superconductivity in magic-angle graphene superlattices, Nature (London) **556**, 43 (2018).

[2] E. Y. Andrei and A. H. MacDonald, Graphene bilayers with a twist, Nat. Mater. **19**, 1265 (2020).

[3] E. Y. Andrei, D. K. Efetov, P. Jarillo-Herrero, A. H. MacDonald, K. F. Mak, T. Senthil, E. Tutuc, A. Yazdani, and A. F. Young, The marvels of moiré materials, Nat. Rev. Mater. **6**, 201 (2021).

[4] D. M. Kennes, M. Claassen, L. Xian, A. Georges, A. J. Millis, J. Hone, C. R. Dean, D. N. Basov, A. N. Pasupathy, and A. Rubio, Moiré heterostructures as a condensed-matter quantum simulator, Nat. Phys. **17**, 155 (2021).

[5] A. Ghiotto, E.-M. Shih, G. S. S. G. Pereira, D. A. Rhodes, B. Kim, J. Zang, A. J. Millis, K. Watanabe, T. Taniguchi, J. C. Hone, L. Wang, C. R. Dean, and A. N. Pasupathy, Quantum criticality in twisted transition metal dichalcogenides, Nature (London) **597**, 345 (2021).

[6] T. Li, S. Jiang, L. Li, Y. Zhang, K. Kang, J. Zhu, K. Watanabe, T. Taniguchi, D. Chowdhury, L. Fu, J. Shan, and K. F. Mak, Continuous Mott transition in semiconductor moiré superlattices, Nature (London) **597**, 350 (2021).

[7] E. Tang and L. Fu, Strain-induced partially flat band, helical snake states and interface superconductivity in topological crystalline insulators, Nat. Phys. **10**, 964 (2014).

[8] J. W. F. Venderbos and L. Fu, Interacting Dirac fermions under a spatially alternating pseudomagnetic field: Realization of spontaneous quantum Hall effect, Phys. Rev. B **93**, 195126 (2016).

[9] J. Mao, S. P. Milovanović, M. Andelković, X. Lai, Y. Cao, K. Watanabe, T. Taniguchi, L. Covaci, F. M. Peeters, A. K. Geim, Y. Jiang, and E. Y. Andrei, Evidence of flat bands and correlated states in buckled graphene superlattices, Nature (London) **584**, 215 (2020).

[10] G. Möller and N. R. Cooper, Composite fermion theory for bosonic quantum Hall states on lattices, Phys. Rev. Lett. **103**, 105303 (2009).

[11] T. Neupert, L. Santos, C. Chamon, and C. Mudry, Fractional quantum Hall states at zero magnetic field, Phys. Rev. Lett. **106**, 236804 (2011).

[12] D. N. Sheng, Z.-C. Gu, K. Sun, and L. Sheng, Fractional quantum Hall effect in the absence of Landau levels, Nat. Commun. **2**, 389 (2011).

[13] N. Regnault and B. A. Bernevig, Fractional Chern insulator, Phys. Rev. X **1**, 021014 (2011).

[14] E. Tang, J.-W. Mei, and X.-G. Wen, High-temperature fractional quantum Hall states, Phys. Rev. Lett. **106**, 236802 (2011).

[15] R. Sohal, L. H. Santos, and E. Fradkin, Chern-Simons composite fermion theory of fractional Chern insulators, Phys. Rev. B **97**, 125131 (2018).

[16] R. Sohal and E. Fradkin, Intertwined order in fractional Chern insulators from finite-momentum pairing of composite fermions, Phys. Rev. B **101**, 245154 (2020).

[17] E. M. Spanton, A. A. Zibrov, H. Zhou, T. Taniguchi, K. Watanabe, M. P. Zaletel, and A. F. Young, Observation of fractional Chern insulators in a van der Waals heterostructure, Science **360**, 62 (2018).

[18] Y. Xie, A. T. Pierce, J. M. Park, D. E. Parker, E. Khalaf, P. Ledwith, Y. Cao, S. H. Lee, S. Chen, P. R. Forrester, K. Watanabe, T. Taniguchi, A. Vishwanath, P. Jarillo-Herrero, and A. Yacoby, Fractional Chern insulators in magic-angle twisted bilayer graphene, Nature (London) **600**, 439 (2021).

[19] H. W. Jiang, H. L. Stormer, D. C. Tsui, L. N. Pfeiffer, and K. W. West, Transport anomalies in the lowest Landau level of two-dimensional electrons at half-filling, Phys. Rev. B **40**, 12013 (1989).

[20] B. I. Halperin, P. A. Lee, and N. Read, Theory of the half filled Landau level, Phys. Rev. B **47**, 7312 (1993).

[21] G. Moore and N. Read, Nonabelions in the fractional quantum Hall effect, Nucl. Phys. B **360**, 362 (1991).

[22] E. Fradkin, C. Nayak, A. Tsvelik, and F. Wilczek, A Chern-Simons effective field theory for the Pfaffian quantum Hall state, Nucl. Phys. B **516**, 704 (1998).

[23] N. Read and D. Green, Paired states of fermions in two-dimensions with breaking of parity and time reversal symmetries, and the fractional quantum Hall effect, Phys. Rev. B **61**, 10267 (2000).

[24] M. Banerjee, M. Heiblum, V. Umansky, D. E. Feldman, Y. Oreg, and A. Stern, Observation of half-integer thermal Hall conductance, Nature (London) **559**, 205 (2018).

[25] M. P. Lilly, K. B. Cooper, J. P. Eisenstein, L. N. Pfeiffer, and K. W. West, Evidence for an anisotropic state of two-dimensional electrons in high Landau levels, Phys. Rev. Lett. **82**, 394 (1999).

[26] R. Du, D. Tsui, H. Stormer, L. Pfeiffer, K. Baldwin, and K. West, Strongly anisotropic transport in higher two-dimensional Landau levels, Solid State Commun. **109**, 389 (1999).

[27] E. Fradkin and S. A. Kivelson, Liquid-crystal phases of quantum Hall systems, Phys. Rev. B **59**, 8065 (1999).

[28] K. B. Cooper, M. P. Lilly, J. P. Eisenstein, L. N. Pfeiffer, and K. W. West, Onset of anisotropic transport of two-dimensional electrons in high Landau levels: Possible isotropic-to-nematic liquid-crystal phase transition, Phys. Rev. B **65**, 241313(R) (2002).

[29] E. Fradkin, S. A. Kivelson, M. J. Lawler, J. P. Eisenstein, and A. P. Mackenzie, Nematic Fermi fluids in condensed matter physics, Annu. Rev. Condens. Matter Phys. **1**, 153 (2010).

[30] Y. You, G. Y. Cho, and E. Fradkin, Theory of nematic fractional quantum Hall states, Phys. Rev. X **4**, 041050 (2014).

[31] N. Karthik and R. Narayanan, Scale invariance of parity-invariant three-dimensional QED, Phys. Rev. D **94**, 065026 (2016).

[32] N. Karthik and R. Narayanan, No evidence for bilinear condensate in parity-invariant three-dimensional QED with massless fermions, Phys. Rev. D **93**, 045020 (2016).

[33] S. M. Chester and S. S. Pufu, Towards bootstrapping QED$_3$, J. High Energy Phys. 08 (2016) 19.

[34] D. Poland, S. Rychkov, and A. Vichi, The conformal bootstrap: Theory, numerical techniques, and applications, Rev. Mod. Phys. **91**, 015002 (2019).

[35] N. Karthik and R. Narayanan, Numerical determination of monopole scaling dimension in parity-invariant three-dimensional noncompact QED, Phys. Rev. D **100**, 054514 (2019).

[36] X. Y. Xu, Y. Qi, L. Zhang, F. F. Assaad, C. Xu, and Z. Y. Meng, Monte carlo study of lattice compact quantum electrodynamics with fermionic matter: The parent state of quantum phases, Phys. Rev. X **9**, 021022 (2019).

[37] S. Albayrak, R. S. Erramilli, Z. Li, D. Poland, and Y. Xin, Bootstrapping $N_f = 4$ conformal qed$_3$, Phys. Rev. D **105**, 085008 (2022).

[38] Y.-C. He, J. Rong, and N. Su, Conformal bootstrap bounds for the $U(1)$ Dirac spin liquid and $N = 7$ Stiefel liquid, SciPost Phys. **13**, 014 (2022).

[39] J. Y. Lee, C. Wang, M. P. Zaletel, A. Vishwanath, and Y.-C. He, Emergent multi-flavor QED$_3$ at the plateau transition between fractional Chern insulators: Applications to graphene heterostructures, Phys. Rev. X **8**, 031015 (2018).

[40] S. M. Girvin, Particle-hole symmetry in the anomalous quantum Hall effect, Phys. Rev. B **29**, 6012 (1984).

[41] B. I. Halperin, The half-full Landau level, in *Fractional Quantum Hall Effects: New Developments* (World Scientific, Singapore, 2020), pp. 79–132.

[42] F. Wilczek, Magnetic flux, angular momentum, and statistics, Phys. Rev. Lett. **48**, 1144 (1982).

[43] J. K. Jain, Composite-fermion approach for the fractional quantum Hall effect, Phys. Rev. Lett. **63**, 199 (1989).

[44] S. C. Zhang, T. H. Hansson, and S. Kivelson, Effective-field-theory model for the fractional quantum Hall effect, Phys. Rev. Lett. **62**, 82 (1989).

[45] A. López and E. Fradkin, Fractional quantum Hall effect and Chern-Simons gauge theories, Phys. Rev. B **44**, 5246 (1991).

[46] D. T. Son, Is the composite fermion a Dirac particle? Phys. Rev. X **5**, 031027 (2015).

[47] C. Wang and T. Senthil, Dual Dirac liquid on the surface of the electron topological insulator, Phys. Rev. X **5**, 041031 (2015).

[48] M. A. Metlitski and A. Vishwanath, Particle-vortex duality of two-dimensional Dirac fermion from electric-magnetic duality of three-dimensional topological insulators, Phys. Rev. B **93**, 245151 (2016).

[49] N. Seiberg, T. Senthil, C. Wang, and E. Witten, A duality web in 2 + 1 dimensions and condensed matter physics, Ann. Phys. **374**, 395 (2016).

[50] A. Karch and D. Tong, Particle-vortex duality from 3D bosonization, Phys. Rev. X **6**, 031043 (2016).

[51] D. F. Mross, J. Alicea, and O. I. Motrunich, Symmetry and duality in bosonization of two-dimensional Dirac fermions, Phys. Rev. X **7**, 041016 (2017).

[52] J.-Y. Chen, J. H. Son, C. Wang, and S. Raghu, Exact boson-fermion duality on a 3D Euclidean lattice, Phys. Rev. Lett. **120**, 016602 (2018).

[53] H. Goldman and E. Fradkin, Loop models, modular invariance, and three dimensional bosonization, Phys. Rev. B **97**, 195112 (2018).

[54] J. H. Son, J.-Y. Chen, and S. Raghu, Duality web on a 3D Euclidean lattice and manifestation of hidden symmetries, J. High Energy Phys. 06 (2019) 038.

[55] P. R. Thomas and M. Stone, Nature of the phase transition in a non-linear O(2)$_3$ model, Nucl. Phys. B **144**, 513 (1978).

[56] M. E. Peskin, Mandelstam 't Hooft duality in Abelian lattice models, Ann. Phys. **113**, 122 (1978).

[57] C. Dasgupta and B. I. Halperin, Phase transition in a lattice model of superconductivity, Phys. Rev. Lett. **47**, 1556 (1981).

[58] P. D. Ye, D. Weiss, R. R. Gerhardts, M. Seeger, K. von Klitzing, K. Eberl, and H. Nickel, Electrons in a periodic magnetic field induced by a regular array of micromagnets, Phys. Rev. Lett. **74**, 3013 (1995).

[59] K. W. Edmonds, B. L. Gallagher, P. C. Main, N. Overend, R. Wirtz, A. Nogaret, M. Henini, C. H. Marrows, B. J. Hickey, and S. Thoms, Magnetoresistance oscillations due to internal Landau band structure of a two-dimensional electron system in a periodic magnetic field, Phys. Rev. B **64**, 041303(R) (2001).

[60] J. Dong, J. Wang, and L. Fu, Dirac electron under periodic magnetic field: Platform for fractional Chern insulator and generalized Wigner crystal, arXiv:2208.10516.

[61] T. Wang, N. F. Q. Yuan, and L. Fu, Moiré surface states and enhanced superconductivity in topological insulators, Phys. Rev. X **11**, 021024 (2021).

[62] M. Hermele, T. Senthil, and M. P. A. Fisher, Algebraic spin liquid as the mother of many competing orders, Phys. Rev. B **72**, 104404 (2005).

[63] S. Gukov, RG flows and bifurcations, Nucl. Phys. B **919**, 583 (2017).

[64] C.-J. Lee and M. Mulligan, Scaling and diffusion of Dirac composite fermions, Phys. Rev. Res. **2**, 023303 (2020).

[65] E. Fradkin and S. Kivelson, Modular invariance, self-duality and the phase transition between quantum Hall plateaus, Nucl. Phys. B **474**, 543 (1996).

[66] W.-H. Hsiao and D. T. Son, Duality and universal transport in mixed-dimension electrodynamics, Phys. Rev. B **96**, 075127 (2017).

[67] W. Chen, M. P. A. Fisher, and Y.-S. Wu, Mott transition in an anyon gas, Phys. Rev. B **48**, 13749 (1993).

[68] W. Rantner and X.-G. Wen, Spin correlations in the algebraic spin liquid: Implications for high-T_c superconductors, Phys. Rev. B **66**, 144501 (2002).

[69] S. Chester and S. Pufu, Anomalous dimensions of scalar operators in QED$_3$, J. High Energy Phys. 08 (2016) 069.

[70] S. L. Sondhi, S. M. Girvin, J. P. Carini, and D. Shahar, Continuous quantum phase transitions, Rev. Mod. Phys. **69**, 315 (1997).

[71] K. Damle and S. Sachdev, Nonzero-temperature transport near quantum critical points, Phys. Rev. B **56**, 8714 (1997).

[72] H. Goldman, M. Mulligan, S. Raghu, G. Torroba, and M. Zimet, Two-dimensional conductors with interactions and disorder from particle-vortex duality, Phys. Rev. B **96**, 245140 (2017).

[73] P. Goswami, H. Goldman, and S. Raghu, Metallic phases from disordered (2+1)-dimensional quantum electrodynamics, Phys. Rev. B **95**, 235145 (2017).

[74] A. Thomson and S. Sachdev, Quantum electrodynamics in 2+1 dimensions with quenched disorder: Quantum critical states with interactions and disorder, Phys. Rev. B **95**, 235146 (2017).

[75] H. Goldman, A. Thomson, L. Nie, and Z. Bi, Collusion of interactions and disorder at the superfluid-insulator transition: A dirty 2D quantum =critical point, Phys. Rev. B **101**, 144506 (2020).

[76] P. Kumar, Y. B. Kim, and S. Raghu, Self-duality of the integer quantum Hall to insulator transition: Composite fermion description, Phys. Rev. B **100**, 235124 (2019).

[77] C.-J. Lee, P. Kumar, and M. Mulligan, Composite fermion nonlinear sigma models, Phys. Rev. B **104**, 125119 (2021).

[78] A. M. M. Pruisken, On localization in the theory of the quantized Hall effect: A two-dimensional realization of the θ vacuum, Nucl. Phys. B **235**, 277 (1984).

[79] A. M. M. Pruisken, Dilute instanton gas as the precursor to the integral quantum Hall effect, Phys. Rev. B **32**, 2636 (1985).

[80] H. Goldman, R. Sohal, and E. Fradkin, Non-Abelian fermionization and the landscape of quantum Hall phases, Phys. Rev. B **102**, 195151 (2020).

[81] A. Lopez and E. Fradkin, Universal structure of the edge states of the fractional quantum Hall states, Phys. Rev. B **59**, 15323 (1999).